Journal of the Industrial Technology Research Institute,
Korea Maritime University, Vol. 9, 1991.

A Discussion on the Optimal Design of a Regenerative Heat Exchanger for Closed Cycle MHD Power Generation

Yoon-Sik Kim *

클로즈드 사이클 MHD 發電用 축열형 열교환기의 最適설계에 관한고찰

金 潤 植

초 록

MHD발전이란, 도전성의 유체를 강력한 자장공간속에 고속으로 통과시킬때 유기되는 기전력을 이용하여 외부 부하에 전력을 공급하는 것으로, 50%를 넘는 에너지 변환효율로 최근 주목을 받고 있는 직접발전의 한분야이다. 발전형태를 분류하면, 이용되는 작동 유체의 종류에 따라 연소가스를 직접 작동유체로 이용하는 오픈 사이클 MHD 발전과 헬륨, 아르곤등의 불활성가스를 작동유체로 이용하는 클로즈드 사이클 MHD 발전으로 크게 구분된다.

본고에서는 클로즈드 사이클 MHD 발전장치의 주요 요소중의 하나인 축열형 열교환기를 연구대상으로 하여, 각 운전모드에 따른 열특성을 고찰하기 위한 모델링법과 그 열특성계산 결과로부터, 양질의 작동유체를 얻기 위한 방책 및 이를 실현하기 위한 축열형 열교환기의 설계법등을 검토한다.

1. Introduction

In a closed cycle MHD power generation system, regenerative heat exchangers are used for heating the working inert gas (argon or helium) up to a temperature of 1650℃, while the impurity level in the working gas is kept below 100 ppm.

In the heat exchanger concerned here, combustion gas and the inert gas pass through the same heat storage bed alternately. Thus multiple heat exchangers are required to supply high

* 한국해양대학 기관공학과 조교수

temperature inert gas to an MHD power generator continuously. To suppress mixing of comustion gas and inert gas, each heat exchanger has to be operated in cycle for four operational periods, 1) heating the heat storage bed by combustion gas, 2) evacuation of the residual combustion gas inside the heat exchanger, 3) heating the inert gas by the heat storage bed, and 4) recovery of the residual inert gas inside the heat exchanger. Therefore, the heat transfer processes inside the heat exchanger are practically unsteady, and an unsteady heat transfer analysis is required to be performed for optimum designing of the heat exchanger.

A regenerative heat exchanger consists of a combustion chamber and a heat storage bed. An unsteady heat transfer analysis regarding the heat storage bed (pebble bed) has been reported in ref.[1] In this paper, an unsteady heat transfer analysis for the combustion chamber is performed firstly, where emphasis is laid on the modeling of the radiative heat transfer.

The analytical results are compared with the experimental data obtained from a pebble bed regenerative heat exchanger for argon heating. Next, this heat transfer analysis code for the combustion chamber is coupled with that for the heat storage bed to simulate the whole thermal performance of the heat exchanger under the comtinuous cyclic operation. On the basis of these analyses, optimum designing of the heat exchanger is discussed to accomplish a higher average temperature and a lower temperature swing of the inert gas at the inlet of MHD power generator.

2. Experinental Facility and Procedure

The structure of the pebble bed regenerative heat exchanger used for experiments is shown in Fig. 1. It consists of three major parts ; the heat storage bed (diameter : 1. 1m, height : 3m) which is filled with alumina pebbles (diameter : 20mm), the combustion chamber, and four-layered insulating wall (width : 0.25m). The total length of the combustion chamber is 2.3m, and a burner is installed at the central uppermost portion of it. Natural gas is supplied to the combustion chamber through the fuel nozzle located at the center of the burner, and is combusted by pre-heated air (250℃) supplied through the tapered air nozzles located around the fuel nozzle.

The combustion gas passes through the pebble bed for about 30 hours, and the top of the pebble bed is heated up to a temperature of about 1850℃ at the end of this heating period. After that, combustion gas inside the heat exchanger is evacuated for about 5 minutes, and then, cold argon is blown from the bottom of the bed for about 2 minutes. This argon is heated up to about 1800℃ in the pebble bed, and is introduced to an MHD generator. The temperature change with time at the top of pebble bed is measured by a platinum-rhodium thermo-couple(20%-40%)from the start of the heating period to the end of the argon heating period.

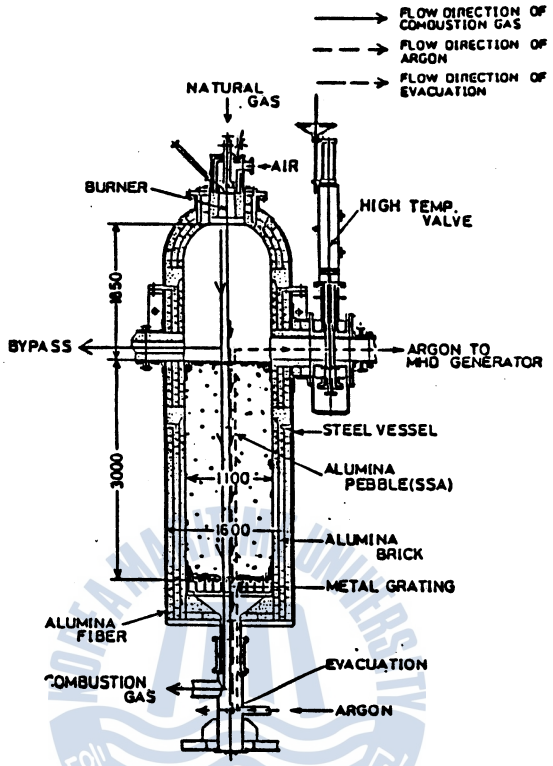

Fig.1 Pebble bed regenerative heat exchanger

In the numerical analysis, the steady state temperature and flow fields in the combustion chamber at the end of the heating period is obtained at first. Then, taking this temperature field as a initial condition, an unsteady heat transfer analysis is performed for the evacuationd and argon heating periods.

3. Basic Equations and Numerical Method

3.1 Analysis Inside the Combustion Chamber

The flow fields regarding the heating and argon heating periods are described by the following two-dimensional steady elliptic differential equation in terms of the dependent variable in the axi -symmetric cylindrical co-ordinate[2].

$$a\left\{\frac{\partial}{\partial z}\left(\varphi\frac{\partial\psi}{\partial r}\right)-\frac{\partial}{\partial r}\left(\varphi\frac{\partial\psi}{\partial z}\right)\right\}-\frac{\partial}{\partial z}\left\{b\frac{\partial}{\partial z}(c\varphi)\right\}-\frac{\partial}{\partial r}\left\{b\frac{\partial}{\partial r}(c\varphi)\right\}+d=0\ (1)$$

Table 1 shows each dependent variables and its related coefficients. The dependent variables to

be solved for the heating period are the stream function, the vorticity, the swirl velocity, the fuel mass fraction, the air mass fraction, and the enthalpy, whereas those for the argon heating period are the stream function, the vorticity and the enthalpy. Since the main heat transfer process is supposed to be the heat radiation rather than the convection, a simple turbulence model[2] is employed in the present study, which is given below.

Table 1. Dependent variables and their coefficients

	φ	a	b	c	d
1.	$\frac{\omega}{r}$	r^2	r^3	μ_t	$\bar{d}$
2.	ψ	0	$\frac{1}{\rho r}$	1	$-\omega$
3.	$rV\theta$	1	$\mu_t r^3$	$\frac{1}{r^2}$	0
4.	m_f	1	$\Gamma_{ft} r$	1	$-rS_f$
5.	m_o	1	$\Gamma_{ot} r$	1	$-rS_o$
6.	i	1	$\Gamma_{it} r$	1	rS_i

$$\bar{d}=-r\frac{\partial}{\partial z}(\rho v_\theta^2)-r^2\left\{\frac{\partial}{\partial z}\left(\frac{u^2+v^2}{2}\right)\frac{\partial P}{\partial r}-\frac{\partial}{\partial r}\left(\frac{u^2+v^2}{2}\right)\frac{\partial p}{\partial z}\right\}$$

$$\mu_t=kD^{\frac{2}{3}}L^{-\frac{1}{3}}\rho^{\frac{2}{3}}(m_fU_f^2+m_oU_o^2)^{\frac{1}{3}} \tag{2}$$

The turbulent diffusion coefficients appeared in the equations for the mass fraction and the enthalpy are defined as follows;

$$\Gamma_{jt}=\frac{\mu_t}{\rho_{jt}} \tag{3}$$

$$\Gamma_{it}\frac{\mu_t}{\rho_{it}} \tag{4}$$

where subscript j represents fuel f or air o, and both the turbulent Schmidt number and the turbulent Prandtl number are assumed to be 1. 0.

The temperature of the insulating wall is evaluated by the following equation.

$$h_wA_{wo}(T_w-T_o)+A_{gw}\varepsilon_w\sigma T_w^4 = h_{gw}A_{gw}(T_g-T_w)+Q_{rin} \tag{5}$$

The first and the second terms on the left-hand side represent the heat conduction through the insulation wall and the radiative heat emission, respectively. The first and the second terms on the right-hand side represent the convective heat transfer between the gas and the wall, and the radiative heat flux from other wall or gas zones, respectively. The convective heat transfer coefficient hgw is evaluated by the following equation[3].

$$Nu=0.023Re^{0.8}Pr^{\frac{1}{3}} \tag{6}$$

The chemical reaction associated with the combustion process of natural gas is assumed to be a single-step chemical reaction whose reaction rate is given by the following Arrhenius expression[4].

$$R_c = A_c e^{-\frac{E_a}{RT}} [m_f]^a [m_o]^b \tag{7}$$

Conditions for the calculation and the coefficients appeared in eq.(7) are summarized in Table 2. A grid configuration for the calculation is shown in Fig.2. Here, the hemispherical shape of the dome section is approximated by the cylindrical one. The right-half side shows the grid spacing for the flow field calculation and the left-half side shows the zone division configuration for the radiation calculation.

Table 2. Used coefficients and conditions

Condition for combustion	
Fuel mass flow rate	: 0.014kg/s
Air mass flow rate	: 0.236kg/s
Inlet air temp.	: 250℃
Inlet fuel temp.	: 25℃
Insulater outer wall temp.	: 230℃.
Combustion gas pressure	: 0.13Mpa
Used constants	
Coeff. for turbulent viscosity k	: 0.012
Collision frequency factor A_c	: 2.8×10^9
Activation energy(Kcal/mol) E_a	: 48.4
Const. for chemical reaction a	: −0.3
Const. for chemical reaction b	: 1.3

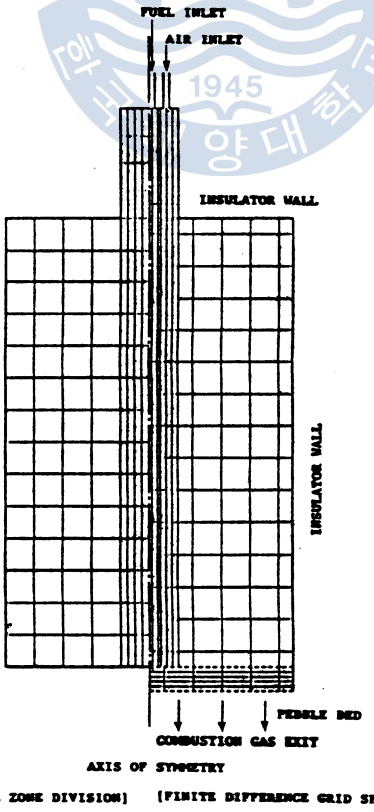

Fig 2. Grid configuration for the calculation

3.2 Radiation Modeling of the Radiative Heat Transfer

In the enthalpy equation for the heating period, the source term S_i is expressed as follows;

$$S_i = R_c \Delta H_c + S_r \tag{8}$$

where the first term on the right-hand side represents the generation of heat by the chemical reaction and the second term represents the net enthalpy change by the radiative heat transfer, respectively.

The combustion chamber is divided into some gas zones and wall zones so as to apply the zone method propesed by Hottel et al[5].

The radiative heat transfer term S_r for the gas zone k, whose volume is V_k, is expressed as follows.

$$\begin{aligned} S_r V_k = & -4 \sum_{n=1}^{3} a_n(T_k)\, k_n V_k \sigma T^4{}_k \\ & + 4 \sum_{n=1}^{3} \sum_{j} a_n(T_j)\, k_n V_j (f_{jk})_n \sigma T^4{}_j \\ & + \sum_{n=1}^{3} \sum_{i} a_n(T_i)\, A_i \varepsilon_i (f_{ik})_n \sigma T^4{}_i \end{aligned} \tag{9}$$

The first, the second and the third terms on the right-hand side are the radiative emission from the zone k, the amount of radiation received from all gas zones V_j and the amount of radiation received from all surface zones A_i, respectively. The combustion gas is represented by a mixture of three grey gases with different absorption coefficient k and a clear gas [5], and an 'and a are weighting factors for the gas emissivity and the absorptivity, respectively. In eq.(9), $(f_{ij})_n$ is the radiative exchange factor for each grey gas and is calculated by the Monte Carlo method[6,7].

Fig.3 shows the distribution of f_{ij} for the three grey gases with different absorption coefficient, where a number of radiative particles are emitted from the upper wall zone enclosed by the bold rectangle. As the absorption coefficient becomes smaller, the radiative energy is shown to spread more evenly in the combustion chamber.

3.3 Analysis Inside the Pebble Bed and Insulating Wall

The heat transfer equations between the gas and the pebbles inside the pebble bed can be expressed as follows[1].

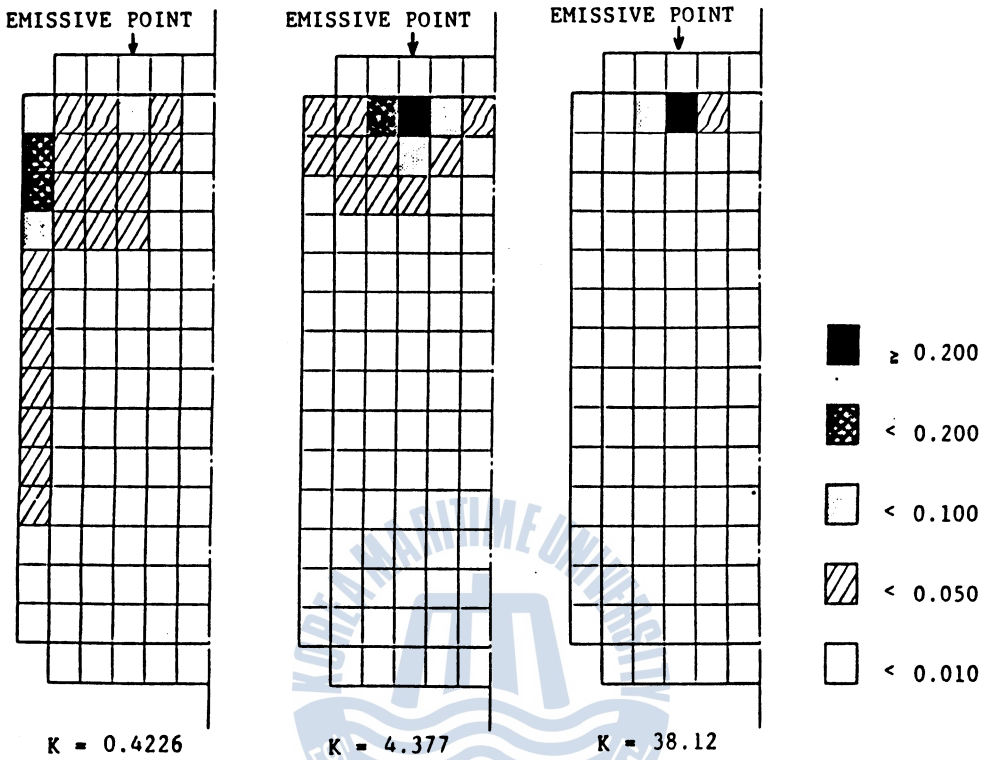

Fig 3. Distribution of $(f_{ij})_n$ for the three grey gases with different absorption coefficient

$$-\dot{m}c_g\frac{\partial T_g}{\partial z}=h_{gp}A_{gp}(T_g-T_p) \tag{10}$$

$$(1-\alpha)\rho_p c_p\frac{\partial T_p}{\partial t}=h_{gp}A_{gp}(T_g-T_p)+k_p\frac{\partial^2 T_p}{\partial z^2} \tag{11}$$

Here, the convective heat transfer between the gas and pebbles and the axial heat conduction in the pebble bed are taken into account.

Regarding the upper and side insulating wall, the flowing unsteady heat conduction equations are employed.

$$\rho_w c_w\frac{\partial T_w}{\partial t}=k_w\frac{\partial^2 T_w}{\partial z^2} \tag{12}$$

$$\rho_w c_w\frac{\partial T_w}{\partial t}=k_w\left(\frac{\partial^2 T_w}{\partial r^2}+\frac{1}{r}\frac{\partial T_w}{\partial r}\right) \tag{13}$$

4. Results and Discussions

4.1 Analysis for the Heating Period

Figure 4 shows the flow pattern of combustion gas in the combustion chamber, which indicates a large recirculating flow in it.

Figure 5 shows the temperature distribution in the combusion chamber, and Fig.6 shows the temperature profile of combustion gas inside the combustion chamber. These two figures indicate that the highest temperature zone is located near the center of the combustion chamber, and some temperature drop is observed toward the top of the pebble bed. The predicted pebble temperature at the top of the bed agrees well with the measured data.

Figure 6 suggests that reduction of the height of the combustion chamber causes an increment of the pebble tomperatu at the top of the bed, which will result in a higher exit temperature for argon.

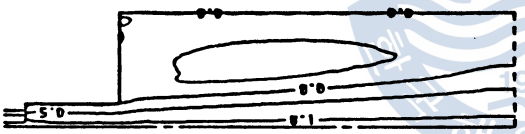

Fig 4. Flow pattern for the combustion gas

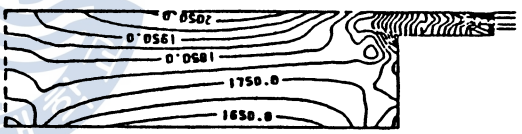

Fig 5. Temperature distribution for the combustion gas

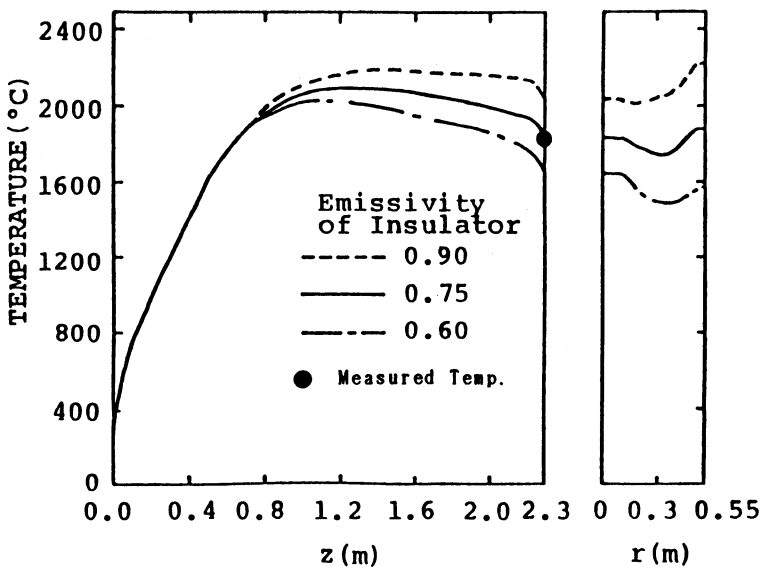

Fig 6. Axial temperature profile in the combustion chamber

4.2 Analysis For the Evacuation and Argon Heating Periods

An unsteady heat transfer analysis for the evacuation period is performed by taking the temperature distributions inside the conbustion chamber obtained above as an initial condition.

In the analysis for the argon heating period, only the temperatures of the insulating wall and the pebble bed are considered to be time-dependent, because their heat capacities are much larger than that of argon.

The calculated and measured temperature changes of pebbles at the top of the bed during the evacuation and argon heating periods are plotted in Fig.7. The calculated argon temperature at the top of the pebble bed is also shown in this figure. The pebble temperature at the top of the bed drops rapidly during the evacuation period because of the radiative heat loss to the lower temperature region of the insulating wall. On the other hand, it rises during the argon heating period because the top of the pebble bed gets heated by argon which has been heated by the highest temperature pebble zone located just below the top surface.

The temperature at the top of the pebble bed during the argon heating period measured by the thermo-couple is supposed to lie between the pebble temperature and the argon temperature at that point. Therefore, Fig.7 shows that the present calculation well explains the measured unsteady temperature change at the top of the pebble bed.

Figure 8 shows the flow patterm of argon. Major fraction of argon gas coming from the pebble bed flows to the exit of the heat exchanger directly, and only a small amount of it circulates

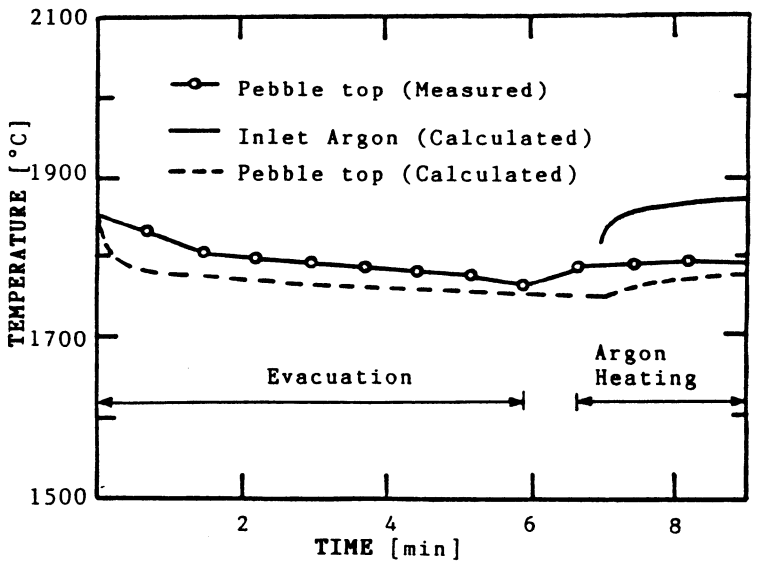

Fig 7. Temperature changes during the evacuation and the argon heating periods

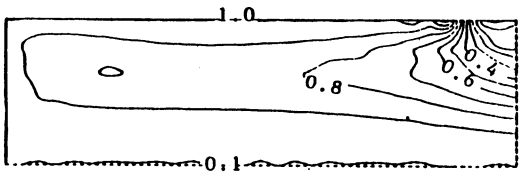

Fig 8. Flow patterm for the argon

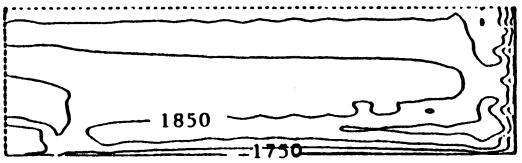

Fig 9. Temperature distribution for the argon

through the combustion chamber to the exit. Fig.9 shows the temperature distribution of argon in the combustion chamber. Its contour seems to be similar to that of the stream line, and a sudden temperature drop can be observed near the insulating wall.

4.3 Unsteady Thermal Performance Under Continuous Cyclic Operation

From the above results, it is comfirmed that the measured unsteady temperature change at the top of the pebble bed in each operational mode can be satisfactorily explained by the present thermal analysis code for the combustion chamber. Nextly, the two thermal analysis codes for the combustion chamber and for the pebble bed are coupled together to caluclate the unsteady thermal performance of the heat exchanger as a whole under the continuous cyclic operation.

Unsteady heat transfer analyses for the four operational periods, that is, 1) heating by combustion gas, 2) evacuation of combustion gas, 3) argon heating, and 4) evacuation of argon are performed repeatedly in cycle until a steady state cyclic solution can be obtained. Here, to simulate the cyclic operation, the initial temperature distributions in the combustion chamber and in the pebble bed for each operational period are given by the ones at the end of the preceding operational period. The conditions assumed in the analysis are shown in Table 3.

Figure 10 shows the temperature change for the pebbles at the top of the bed(dotted line) and also that for argon at the exit of the heat exchanger(solid line), during one operational cycle. The temperature of the pebble at the top of the bed falls during each evacuation period and rises in the heating period. At the end of the evacuation of combustion gas, the temperature of pebbles at the top of the bed is found lower than that at a location of about 10cm below the top because of radiative heat loss. Therefore, during the

Table 3. Conditions assumed in the calculation for the continuous cyclic operation

Combustion chamber height	2.5m
Pebble bed height	3.0m
Mass flow of combustion gas	2.3kg/m²s
Mass flow of argon	6.3kg/m²s
Time lenght of combustion gas heating period	300s
Time length of combustion gas evacuating period	150s
Time length of argon heating period	300s
Time length of argon recovery period	150s
Inlet temperature of argon	27℃
Pressure of combustion gas	0.13Mpa
Pressure of argon	0.8Mpa

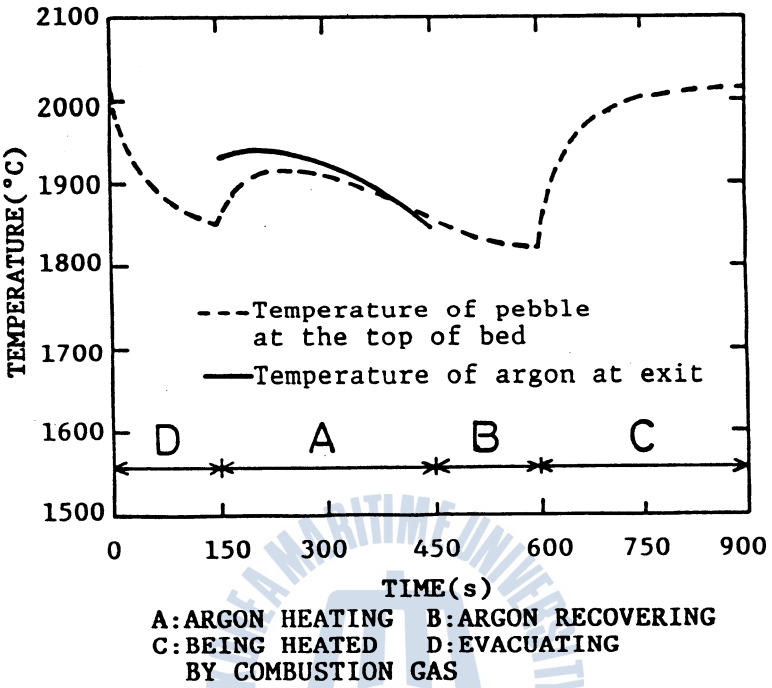

Fig 10. Temperature changes of argon and the pebbles at the top of the bed during one operational cycle

argon heating period, the temperatures of both the pebbles and argon at the top of the bed rise at first. Then they begin to fall because the pebble bed loses its enthalpy as argon passes through it.

4.4 Discussions on the Optimum Designing of a Heat Exchanger

Finally, employing the present thermal analysis code, we will discuss the optimum designing of a pebble bed heat exchanger to improve its thermal performance. From the standpoint of an MHD generator, heat exchangers should supply argon flow continuously with average temperature as high as possible while the temperature swing of argon associated with switching heat exchangers should be kept as small as possible.

Here, these two thermal parameters (the average temperature and the temperature swing) are investigated by changing the heights of the combustion chamber and the pebble bed.

Figure 11 shows the average argon temperature and the swing of argon temperature as a function of the height of the combustion chamber, where the pebble bed height is fixed to 3m. While the swing of argon temperature does not strongly depend on the height of the combustion chamber, the average argon temperature drops significantly as the height of the combustion chamber become larger. The reason for lower average temperature in a higher combustion

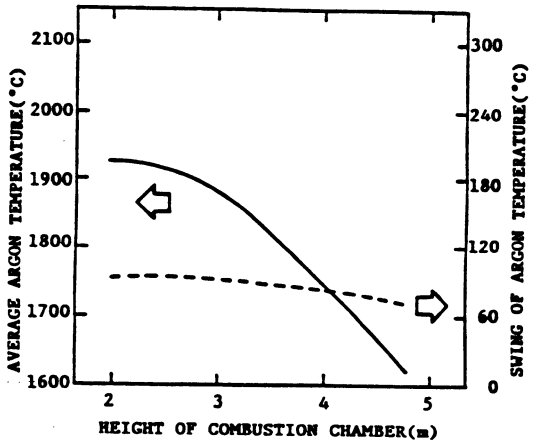

Fig 11. Average argon temperature and argon temperature swing as a function of the height of the combustion chamber

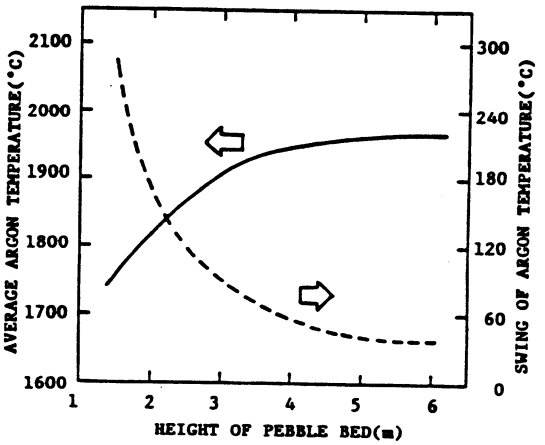

Fig 12. Average argon temperature and argon temperature swing as a function of the height of the pebble bed

chamber is that the distance between the top of the pebble bed and the location of the maximum flame temperature gets longer and the temperature of combustion gas arriving at the top of the bed becomes lower.

Figure 12 shows the results for a different height of the pebble bed, where the height of the combustion chamber is fixed to 2.5m. From this figure, we can see that the swing of argon temperature depends strongly on the height of the pebble bed, and if the bed height is above about 3m, both the average temperature and the temperature swing become less dependent on the height of the pebble bed. This is one of distinctive features of pebble bed type regenerative heat exchangers, which is due to the high heat transfer performance between pebbles and gases.

From the above results, it can be said that a sufficient attention should be paid not only to the heat storage bed but also to the combustion chamber in designing a regenerative heat exchanger.

5. Conclusion

A two-dimensional heat transfer analysis in the combustion chamber of a pebble bed regenerative heat exchanger for high temperature argon heating has been performed for the heating, evacuation and argon heating period. The calculated results well explain the measured temperature change with time at the top of the pebble bed facing the combustion chamber.

This heat transfer analysis code for the combustion chamber has been coupled with that for the heat storage pebble bed to simulate the whole unsteady thermal performance of a heat exchanger under the continuous cyclic operation. The analytical results lead to the conclusion that the geometry optimization both for the combustion chamber and for the heat storage bed is important in order to improve the thermal performance of a regenerative heat exchanger.

References

1) K.Yoshikawa et al., Trans. JSME(in Japanese) Vol. 52-476(B), pp. 1750-1757, 1986
2) Gosman, A.D. et al., Heat and Mass Transfer in Recirculating Flow, Academic Press, London, 1969.
3) JSME Data Book : Heat Transfer 3rd Edition, pp. 28-30, 1975
4) Charles, K.W., Fredrick, L.D., Prog. Energy Com, Sci., Vol. 10, pp. 1-18, 1984
5) Hottel, H.C and Sarofim, A.F., Int. J. Heat Mass Transf., Vol. 8, pp. 1153-1169, 1965.
6) Howell, J.R. and Perlmutter, M., Trans. ASME. J. Heat Transf., Vol. 86, pp. 116-122, 1964.
7) Perlmutter, M. and Howell, J.R., Trans. ASME. J. Heat Transf., Vol. 86, pp. 169-179, 1964.